International Journal of Biological Macromolecules 318 (2025) 145352

Contents lists available at ScienceDirect

International Journal of Biological Macromolecules

journal homepage: www.elsevier.com/locate/ijbiomac

# CircSETD3 interrupts the bidirectional positive feedback of ErbB3 and Akt by sponging miR-4667-5p to inhibit colorectal cancer progression and cetuximab resistance

Xiaomin Li [a,e,1], Tao Chen [b,1], Yujie Cai [a,1], Jingtao Zhang [a], Yuxin Wang [a], Jianjun Wang [d], Xueyuan Mao [c], Liancheng Xu [b], Dongdong Li [a], Yu Wang [a], Xiaoyan Wang [a,*]

[a] Department of Gastroenterology, Clinical Medical Research Center, The Suqian Clinical College of Xuzhou Medical University, Suqian Clinical Medical College of Jiangsu University, 223800 Suqian, Jiangsu Province, China
[b] Department of General Surgery, Jiangsu Provincial People's Hospital Suqian Hospital, 223800 Suqian, Jiangsu Province, China
[c] Department of Pathology, Jiangsu Provincial People's Hospital Suqian Hospital, 223800 Suqian, Jiangsu Province, China
[d] Department of Histology and Embryology, Wannan Medical College, 241002 Wuhu, Anhui Province, China
[e] Department of Pathology, School of Basic Medical Sciences, Southern Medical University, 510515 Guangzhou, Guangdong Province, China

ARTICLE INFO

*Keywords:*
Colorectal cancer
circSETD3
hsa_circ_0000567
miR-4667-5p
ErbB3

ABSTRACT

Circular RNAs play crucial roles in tumor progression and drug resistance. We previously reported that circSETD3 is downregulated in colorectal cancer (CRC) and correlates with tumor size and metastasis; however, the precise biological functions and underlying the mechanisms of action of circSETD3 in CRC remain unclear. Therefore, in the present study, we aimed to investigate the role of circSETD3 in CRC growth, metastasis, and cetuximab resistance using in vitro and in vivo functional assays. Our results demonstrated that circSETD3 acts as a tumor suppressor in CRC progression and cetuximab resistance. Mechanistically, RNA-seq, FISH, dual-luciferase reporter assays, and ChIP assays revealed that reduced circSETD3 expression in CRC activated ErbB3 and its downstream Akt pathway. Notably, we found that the Akt pathway upregulated ErbB3 transcription via HIF1A, indicating the presence of a novel positive feedback loop between ErbB3 and Akt pathway which reinforces CRC progression and drives cetuximab resistance. Furthermore, circSETD3 deficiency in CRC triggered a feedback loop through the miR-4667-5p–RASA4 axis which was effectively suppressed by exosomal circSETD3 supplementation. Thus, our findings highlight circSETD3 to be a promising therapeutic target for inhibiting CRC progression and overcoming cetuximab resistance.

## 1. Introduction

Colorectal cancer (CRC) is one of the most common cancers worldwide and ranks third in morbidity and second in mortality according to the latest cancer statistical analysis [1]. Metastasis and drug resistance are core factors that cause CRC-related deaths. Although anti-epidermal growth factor receptor (anti-EGFR) monoclonal antibodies such as cetuximab and panitumumab prolong the survival of patients with metastatic CRC [2], drug resistance limits their efficacy and restricts their clinical applications [3,4]. Therefore, an urgent need persists to explore the mechanisms underlying the malignant progression of CRC, particularly metastasis and anti-EGFR resistance.

EGFR belongs to the erb-b2 receptor tyrosine kinase (ErbB) family, which contains four members, including ErbB1(EGFR), ErbB2, ErbB3, ErbB4. They combine to form homodimers or heterodimers to activate the downstream Ras and Akt pathways. Cetuximab competitively binds to the extracellular domain of EGFR to prevent the binding of EGFR to its ligand, thereby reducing the transduction of the EGFR pathway and inhibiting cancer cell proliferation, migration, and angiogenesis. As the main downstream effectors of the ErbB family, Ras and Akt are crucial factors determining the efficacy of cetuximab. Studies have demonstrated that the upregulation of other ErbB family members, particularly ErbB2 or ErbB3, contributes to cetuximab resistance by activating the Ras and Akt signaling pathways [5–9]. However, the mechanisms underlying ErbB2 or ErbB3 upregulation in cancer remain unclear.

Circular RNA (circRNAs) are novel transcripts present in almost all

* Corresponding author.
*E-mail address:* 17805296777@163.com (X. Wang).
[1] These authors share first authorship.

https://doi.org/10.1016/j.ijbiomac.2025.145352
Received 19 January 2025; Received in revised form 15 June 2025; Accepted 16 June 2025
Available online 18 June 2025

eukaryocytes, which form a closed-loop structure through back splicing and therefore possesses stability. Recently, an increasing number of studies have shown that circular RNA participates in CRC progression [10,11] and anti-EGFR resistance [12]. For instance, circHIF1A promotes cetuximab resistance in CRC by regulating glycometabolism [13], while circIFNGR2 promotes CRC cell proliferation and migration, and induces cetuximab resistance by upregulating KRAS expression [14]. These findings indicate that circRNAs are potential regulators of the efficacy of anti-EGFR therapy in CRC.

circSETD3 (hsa_circ_0000567) is generated by back-splicing exons 2–6 of SET domain-containing 3 (SETD3). We were the first to report the significant downregulation of circSETD3 in CRC tissues [15]. Subsequent studies have revealed dysregulated circSETD3 expression across multiple cancer types [16–19], suggesting its potential as a pan-cancer regulator. However, the precise biological functions and molecular mechanisms underlying the role of circSETD3 in cancer progression remain largely unknown. Therefore, in the present study, we aimed to investigate the role and mechanisms of circSETD3 in CRC growth, metastasis, and cetuximab resistance using in vitro and in vivo functional assays. Our findings will provide novel insights into the molecular mechanisms underlying CRC development and cetuximab resistance.

## 2. Materials and methods

### 2.1. Cell lines

Human CRC cell lines RKO and HCT116 were obtained from ATCC (Manassas, VA, USA). The culture medium for RKO is MEM (KGL1602–500, KeyGEN, Nanjing, China) and for HCT116 is McCoy's 5 A (KGL1702–500, KeyGEN, Nanjing, China). The medium was supplemented with fetal bovine serum to a final concentration of 10 %. Cells were cultured in a cell incubator with 5 % $CO_2$.

### 2.2. CRC samples

Colon cancer tissues cDNA microarray (HColA095Su02) was purchased from Shanghai Outdo Company (Shanghai, China). The microarray includes 80 cases of colon cancer with clinical information and survival data, which were recorded and archived in the National Engineering Center for Biochip. The use of cDNA microarray for research purposes was approved by the Ethics Committee of Shanghai Outdo Biotech Company. Other 32 cases of CRC fresh tissues used in the research were obtained from the Jiangsu Provincial People's Hospital Suqian Hospital (Suqian, China). Cancer tissues were taken from the resected CRC samples and avoided necrosis. The adjacent noncancerous tissues were taken from the site 5 cm away from the cancers. These tissues were stored at −80 °C until RNA extraction. The paraffin samples were obtained from the pathology department of the Jiangsu Provincial People's Hospital Suqian Hospital. The use of clinical materials for research purposes was approved by the Ethics Committee of Jiangsu Provincial People's Hospital Suqian Hospital (Suqian, China). All patients signed consent forms.

### 2.3. RNA extraction, reverse transcription, and real time quantitative poly chain reaction (RT-qPCR)

These assays were carried out according to our previous reports [10,11]. The reagents used in these experiments are as follows. Total RNA was isolated using RNAiso Plus reagent (#9109, Takara, Japan). Reverse transcription was performed using PrimeScript™ RT reagent Kit with gDNA Eraser (RR047A, Takara, Japan). RT-qPCR was conducted using SybrGreen qPCR Mastermix (DBI2043, DBI Bioscience, Germany) in ABI 7500 Fast Real-Time PCR System or LightCycler-480. The CT values of detected genes were obtained and △CT values were calculated by subtracting the CT values of the internal references GAPDH or β-actin. The relative expression of target genes was shown as $2^{-\triangle CT}$. The primers used in the research were listed in Supplementary Table S1.

### 2.4. siRNA, lentivirus, vector construction, miRNA mimics, and Akt inhibitor

GenePharma (Suzhou, China) or RiboBio (Guangzhou, China) designed and synthesized siRNAs used in the study and the sequences were list in the Supplementary Table S2. The siRNA1 sequence of circSETD3 was used to generate lentivirus vectors targeting circSETD3 (sh-circSETD3) by Genechem (Shanghai, China). circSETD3 overexpression vector was generated using pCD5-ciR plasmid (Geneseed Biotech, Guangzhou, China). Ruibiotech (Guangzhou, China) and GENEWIZ (Suzhou, China) constructed all vectors used in the research. All miRNA mimics used in the research were purchased from GenePharma (Suzhou, China). Akt inhibitor (Artemisinin) was purchased from MCE (HY-B0094, State of New Jersey, USA).

### 2.5. CCK8, colony formation, EdU, transwell migration, wound healing assays

These experiments were performed as our previous study [10,11]. The reagents used in these assays are as follows: Cell Counting Kit-8 (C6005, NCM biotech, Suzhou, China). EdU Cell Proliferation Kit with Alexa Fluor 555 was purchased from Epizyme (CX003, Shanghai, China).

### 2.6. RNA-sequence

RNA-seq and bioinformatics analysis were carried out by The Beijing Genomics Institute (BGI, China). The RNA-seq raw data have been deposited in the NCBI Sequence Read Archive (SRA) database (https://www.ncbi.nlm.nih.gov/sra/ PRJNA1181276).

### 2.7. Nude mice xenograft subcutaneous and metastatic tumor model

Four-week-old female BALB/c nude mice were purchased from Guangdong Medical Experimental Animal Center (Guangzhou, China) and all animal experimental protocols were approved by the Animal Care and Use Committee of Wannan Medical College. For establish subcutaneous tumor models, about $5 \times 10^6$ HCT116 or RKO cells with stable downregulated expression of circSETD3 or control cells were injected subcutaneously into the armpit of mice. Tumor volumes were calculated using the formula (length × $width^2$)/2. For cetuximab treatment experiment, cetuximab (Merck, Germany) was injected intraperitoneally, 20 mg/kg body weight, 2 times a week, for 3 weeks. The tumor volume was calculated with the abovementioned formula. For constructing liver metastasis model, the subcutaneous tumor was cut into 1 $mm^3$ pieces and transplanted into the serous of the caecum. Eight weeks later, the mice were euthanized and the cecal xenograft tumors and livers were resected in order to measure the number of metastases in the liver.

### 2.8. Chromatin immunoprecipitation (ChIP)

ChIP was performed using the SimpleChIP® Enzymatic Chromatin IP Kit (#9003, Cell Signaling Technology, USA) according to the instruction. In short, CRC cells were fixed to make DNA and proteins cross-linked, and lysed after washed and harvested. The lysis was centrifugated to get nuclei pellet. Then, chromatin pellet was digested followed by incubating with HIF1A antibody (1:200 dilution, YT2133, Immunoway, USA) or anti-IgG antibodies at 4 °C overnight. Magnetic beads were used to capture the DNA-protein complexes. After washing and elution, the chromatin was subjected to PCR and RT-qPCR detection with the specific primers for magnifying 117 bp fragment of ErbB3 promoter (forward, 5′- GGTTTCGAGTCTGGGAGA −3′; reverse, 5′-GGTTCACTTGGTGGATTTT −3′).

### 2.9. Fluorescence in situ hybridization (FISH)

FISH was carried out using the Fluorescent in Situ Hybridization Kit (F11101, GenePharma, China) according to the instruction. Briefly, CRC cells in culture plates were fixed, washed, and permeabilized. Then, CRC cells were incubated with Cy3-labeled single stranded DNA oligo probes against circSETD3 (RiboBio, Guangzhou, China) and FAM-labeled miR-4667-5p probes (GenePharma, China) at 37 °C overnight for hybridization reaction. Cells were observed using the laser scanning confocal microscope after DAPI staining nuclei.

### 2.10. Dual- luciferase reporter assay

The dual-luciferase reporter assay was performed by using the Dual Luciferase Reporter Assay System (E1910, Promega, WI, USA) and the Dual Luciferase Reporter Gene Assay Kit (RG027, Beyotime, Shanghai, China). CRC cells were co-transfected with circSETD3, RASA4 3'UTR wild or mutant luciferase reporter vectors and miRNA mimics. After 48 h, cells were lysed and subsequently subjected to detection of luciferase activity and Renilla luciferase activity according to the instruction and our previous study [11].

### 2.11. Western blot

The isolation of total protein and western blot were conducted as our previous research [10,11]. The primary antibodies: anti-ErbB3 (1:1000, YT1608, Immunoway, USA), anti-EGFR (1:1000, R22778, Zenbio, Chengdu, China), anti-Akt (1:1000, R23412, Zenbio, China), anti-p-Akt (Ser473) (1:1000, 66,444–1-lg, Proteintech, USA), anti-RASA4 (1:1000, YN1153, Immunoway, USA), anti-cleaved-caspase3 (1:500, YM3431, Immunoway, USA), anti-cleaved-PARP (1:1000, AB32064, Abcam, UK), anti-β-tubulin (1:2000, 10,094–1-AP, Proteintech, USA), anti-CD9 (1:1000, ab92726, Abcam, UK), anti-CD63 (1:2000, ab217345, Abcam, UK), anti-TSG101 (1:1000, ab125011, Abcam, UK), and anti-Calnexin (1:1000, #2433, Cell Signaling, USA). The second antibodies were HRP-conjugated goat anti-mouse IgG (1:5000, SA00001–1, Proteintech, USA) and goat anti-rabbit IgG (1:5000, SA00001–2, Proteintech, USA).

### 2.12. Immunohistochemistry (IHC)

IHC staining and H-Score calculation of the images for quantitative analysis were performed according to our previous study [10]. The primary antibodies for IHC staining were anti-RASA4 (1:100, 822,975, Zenbio, China), anti-p-Akt (Ser473) (1:100, YP0006, Immunoway, USA), and anti-ErbB3 (1:100, 10,369–1-AP, Proteintech, USA).

### 2.13. Exosome extraction

HCT116 cells were transfected with the circSETD3 overexpression vector for 24 h, then washed and changed for fresh serum-free culture medium. After 24 h, exosomes were isolated from culture medium using Ribo™ Exosome Isolation Reagent (for cell culture media) (C10130, RiboBio, China) according to the instruction. Then, exosome micrographs and nanoparticle tracking analysis for characterizing the exosomes were performed using a transmission electron microscope (Leica Microsystems, Wetzlar, Germany) and NanoSight NS300 (Malvern Panalytical, Malvern, UK) in Huayin (Guangzhou, China).

### 2.14. Statistical analyses

Statistical analysis was conducted by using GraphPad Prism 9.0 (GraphPad Software, La Jolla, CA, USA) and SPSS23.0 software (IBM, USA). The evaluation of the difference between two groups was performed by using a two-tailed Student's *t*-test. The paired t-test was used to detect the difference of circSETD3 expression in CRC samples and adjacent noncancerous samples. The comparison of overall survival time between high and low circSETD3 expression groups was analyzed with Kaplan-Meier method and Log rank test. The correlation between circSETD3 expression and clinicopathological parameters were evaluated using Chi square $\chi 2$ test. The evaluation of prognostic value of circSETD3 was performed using the univariate and multivariate Cox proportional hazards model. A $p < 0.05$ was considered statistically significant, and *N* indicates not significant.

## 3. Results

### 3.1. Downregulation of circSETD3 correlates with poor prognosis in colorectal cancer patients

We previously revealed that circSETD3 is downregulated in CRC tissues, and that lower expression of circSETD3 is positively correlated with tumor size, metastasis, and TNM stage [15]. However, the relationship between circSETD3 expression and the prognosis of patients with CRC remains unknown. In the current study, we further uncovered the prognostic value of circSETD3 using a cDNA microarray containing 80 colon cancer tissue samples. Consistent with our previous study [15], circSETD3 expression was lower in cancer tissues than that in the normal tissues in the 14 paired of cancer tissues and normal tissues in the cDNA microarray (Fig. 1A). We divided the 80 colon cancer tissue samples into a high circSETD3 expression group ($n = 40$) and a low circSETD3 expression group (n = 40) according to the median circSETD3 expression to further confirm the relationship between circSETD3 expression and the clinicopathological parameters of the patients. Statistical analysis revealed that high circSETD3 expression was negatively correlated with lymphatic metastasis and TNM stage, however, no significant relationship was observed with age, sex, cancer differentiation, or serosal invasion (Fig. 1B and Table S3).

Kaplan–Meier survival analysis and univariate and multivariate Cox proportional hazards models were used to evaluate the prognostic value of circSETD3. Kaplan–Meier survival analysis indicated that patients with higher circSETD3 expression had a higher overall survival (OS) rate than those with lower circSETD3 expression (Fig. 1C). Furthermore, a univariate Cox proportional hazards model revealed that low circSETD3 expression increased the risk of death (Fig. 1D). Based on the univariate Cox regression analysis, age, serosal invasion, cancer differentiation, lymphatic metastasis, and circSETD3 expression were selected for multivariate Cox regression analysis, which further confirmed that patients with lower circSETD3 expression had a higher risk of mortality (Fig. 1E). These results indicated that downregulated circSETD3 expression was correlated with poor prognosis in patients with colon cancer, and that circSETD3 was an independent prognostic factor.

### 3.2. circSETD3 downregulation drives malignant progression of colorectal cancer in vitro and in vivo

As the above findings implied that circSETD3 might be involved in CRC growth and metastasis, we performed functional experiments to test this hypothesis. First, we downregulated circSETD3 expression in CRC cells using siRNA targeting circSETD3 (Fig. 2A). CCK8 showed that circSETD3 knockdown boosted the proliferation of CRC cells (Fig. 2B). Similarly, results of the colony formation assay indicated that decreased circSETD3 expression enhanced the ability of CRC cells to form colonies (Fig. 2C). In line with the CCK8 and colony formation assays, EdU staining revealed that the EdU-positive cell rate was higher in the silenced circSETD3 expression group than that in the control group (Fig. 2D). In addition, a Transwell assay was performed to assess the effects of circSETD3 on CRC cell migration. Results demonstrated that the reduced circSETD3 expression increased the number of migrating cells (Fig. 2E). Consistent with the Transwell assay, the wound healing assay also showed that reduced circSETD3 expression increased the migration distance of CRC cells (Fig. 2F). Together, these results

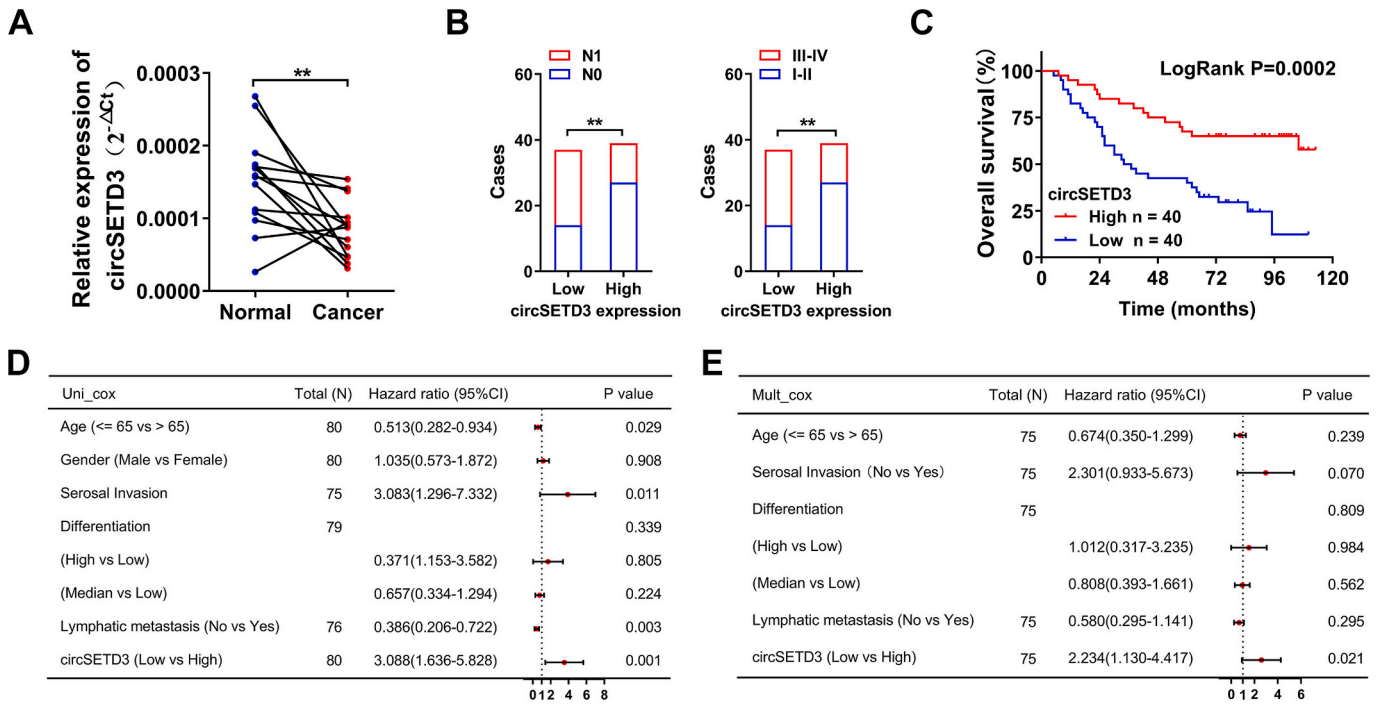


**Fig. 1.** Lower circSETD3 expression indicates poor prognosis.
A) circSETD3 expression was lower in the cancer tissues ($n = 14$) than that in the normal tissues (n = 14) in the colon cancer microarray. B) circSETD3 expression was negatively correlated with lymphatic metastasis (N1) and TNM stage III–IV. C) Log rank test survival analysis indicated that the patients with low circSETD3 expression had a lower overall survival (OS) rate than patients with high circSETD3 expression. D) The univariate Cox proportional hazards model revealed that the lower circSETD3 expression increased the risk of death. E) The multivariate Cox regression analysis verified that lower circSETD3 expression was an independent factor for poor prognosis.

demonstrate that circSETD3 suppresses CRC cell proliferation and migration in vitro.

Subcutaneous xenograft models were then constructed to investigate the effects of circSETD3 on CRC growth in vivo. Representative images and graphs show that tumors with silenced circSETD3 expression were larger than those in the control group (Fig. 2G), demonstrating that circSETD3 deletion promotes CRC cell growth in vivo. Additionally, the influence of circSETD3 on CRC metastasis in vivo was assessed by establishing a cecal xenograft model using CRC cells with the knockdown of circSETD3 expression or control cells. Gross staining and hematoxylin and eosin staining revealed cecal xenografts and metastatic lesions in the liver (Fig. 2H). Calculation of the number of metastases in the liver demonstrated that knockdown of circSETD3 expression increased hepatic metastases (Fig. 2I). Taken together, these results indicate that downregulation of circSETD3 expression promotes the growth and metastasis of CRC.

### 3.3. *circSETD3 overexpression suppresses proliferation and migration in CRC*

We also performed gain-of-function assays. First, circSETD3 expression was upregulated in CRC cells using a circSETD3 overexpression vector (Fig. 3A). CCK8 analysis revealed that overexpression of circSETD3 restrained CRC cell proliferation (Fig. 3B). In addition, the colony formation assay showed that increased circSETD3 expression decreased the number of colonies formed (Fig. 3C). Consistent with the CCK8 and colony formation assays, elevated circSETD3 expression reduced the number of EdU-positive cells (Fig. 3D). Furthermore, the Transwell assay indicated that increasing circSETD3 expression suppressed the motion of CRC cells, resulting in fewer migrating cells across the Transwell (Fig. 3E). Moreover, the wound healing assay showed that upregulated circSETD3 expression impaired the migratory capacity of CRC cells (Fig. 3F). These findings demonstrate that overexpression of circSETD3 suppresses CRC cell proliferation and migration.

### 3.4. *Downregulation of circSETD3 activates the ErbB3/Akt pathway*

Subsequently, RNA-seq was performed using RKO cells with circSETD3 knockdown using two siRNAs targeting circSETD3 to investigate the mechanism of circSETD3 in CRC progression. Compared to the control cells, 489 and 1017 differentially expressed genes were identified in the two siRNA-circSETD3 groups (Fig. 4A). Among them, 229 genes overlapped in both siRNA-circSETD3 groups (Fig. 4B). Kyoto Encyclopedia of Genes and Genomes (KEGG) enrichment analysis based on the 229 genes revealed that circSETD3 was mainly involved in the EGFR tyrosine kinase inhibitor resistance, ErbB, Ras, and PI3K/Akt pathways (Fig. 4C). RNA-seq revealed that ErbB3 and EGFR were upregulated in CRC cells with knockdown of circSETD3 expression (Fig. S1). Since ErbB3 and EGFR are upstream of the enriched pathways, we examined their expression in CRC cells after circSETD3 knockdown or overexpression. The results confirmed that ErbB3 expression was negatively regulated by circSETD3, whereas EGFR expression was not affected by circSETD3 (Fig. 4D). Western blotting further verified that ErbB3 and its downstream target p-Akt were upregulated in RKO and HCT116 cells with knockdown of circSETD3 expression, while they were reduced with circSETD3 overexpression (Fig. 4E). Consistent with the in vitro data, IHC staining demonstrated that circSETD3 knockdown increased ErbB3 and p-Akt levels in xenograft tumors (Fig. 4F and G).

Subsequently, we assessed the relationship between circSETD3 and ErbB3, p-Akt expression in clinical CRC samples. Briefly, we evaluated circSETD3 expression in an cohort of 36 CRC tissue samples and divided them into low and high circSETD3 expression group according to the median expression of circSETD3 (Fig. S2). Immunohistochemical staining revealed that p-Akt and ErbB3 expression levels were higher in the low circSETD3 expression group than in the high circSETD3 expression group (Fig. 4H). These findings indicate that reduced

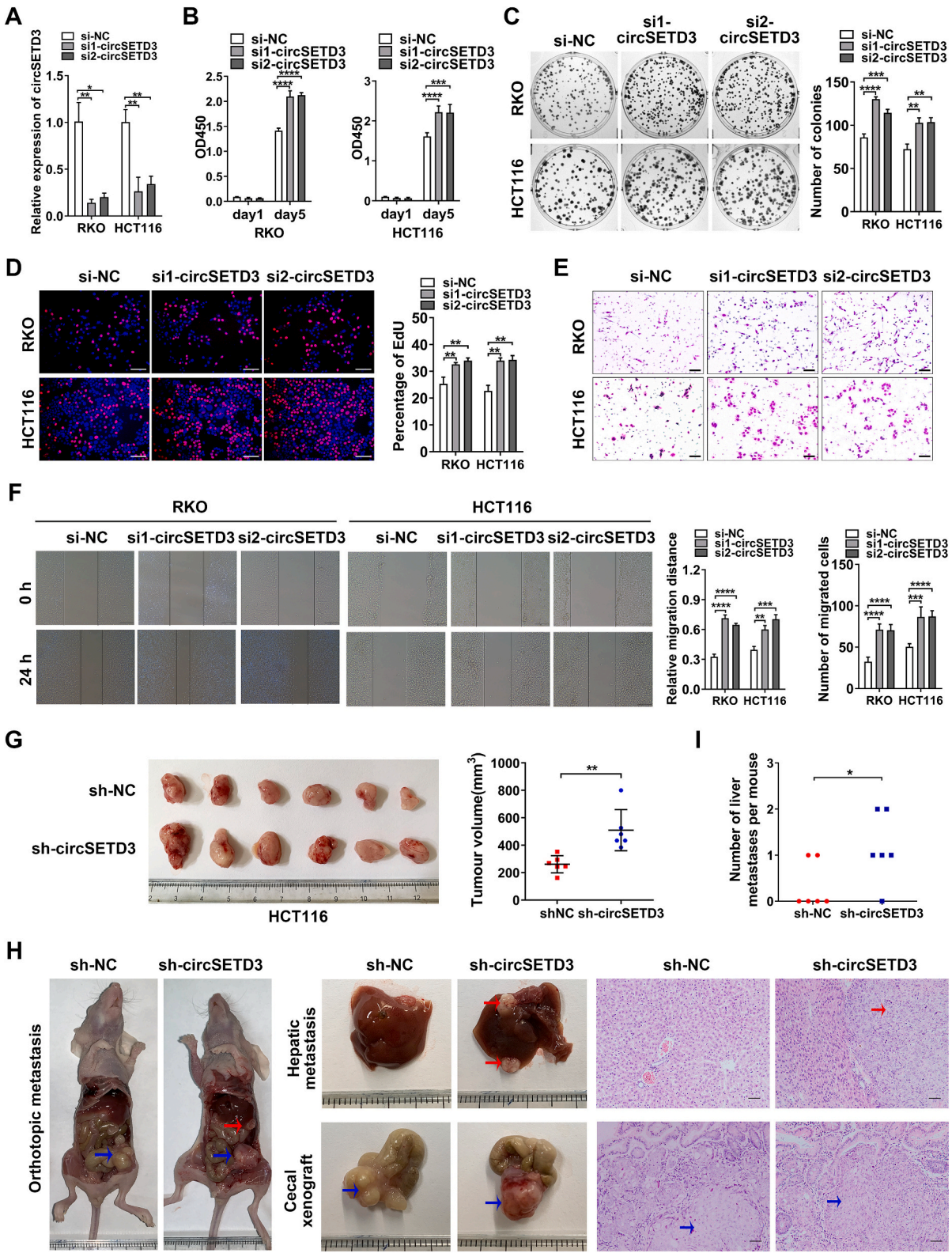


**Fig. 2.** Lower circSETD3 expression promotes the growth and metastasis of CRC cells in vitro and in vivo.
A) circSETD3 expression was downregulated by two siRNAs targeting circSETD3. B) CCK8 showed that circSETD3 knockdown enhanced the viability of CRC cells. C) Colony formation indicated that the decreased circSETD3 expression in CRC cells increased the number of colonies. D) EdU staining showed that the silenced circSETD3 expression reduced the proliferation of CRC cells. Scale bars: 100 μm. E) Transwell assay demonstrated that downregulated circSETD3 expression promoted the migratory capacity of CRC cells. Scale bars: 50 μm. F) Would healing assay revealed that circSETD3 knockdown promoted the migration of CRC cells. Scale bars: 200 μm. G) The representative images and calculated tumor volumes showed that the tumor with silenced circSETD3 expression were larger than that in the control group ($n = 6$). H) The gross and HE staining images showed the cecal xenograft and hepatic metastatic lesion of nude mice. Scale bars: 50 μm. Blue arrows indicate the cecal xenograft tumor and red arrows indicate the hepatic metastatic tumor. I) circSETD3 knockdown increased the number of hepatic metastatic lesion.

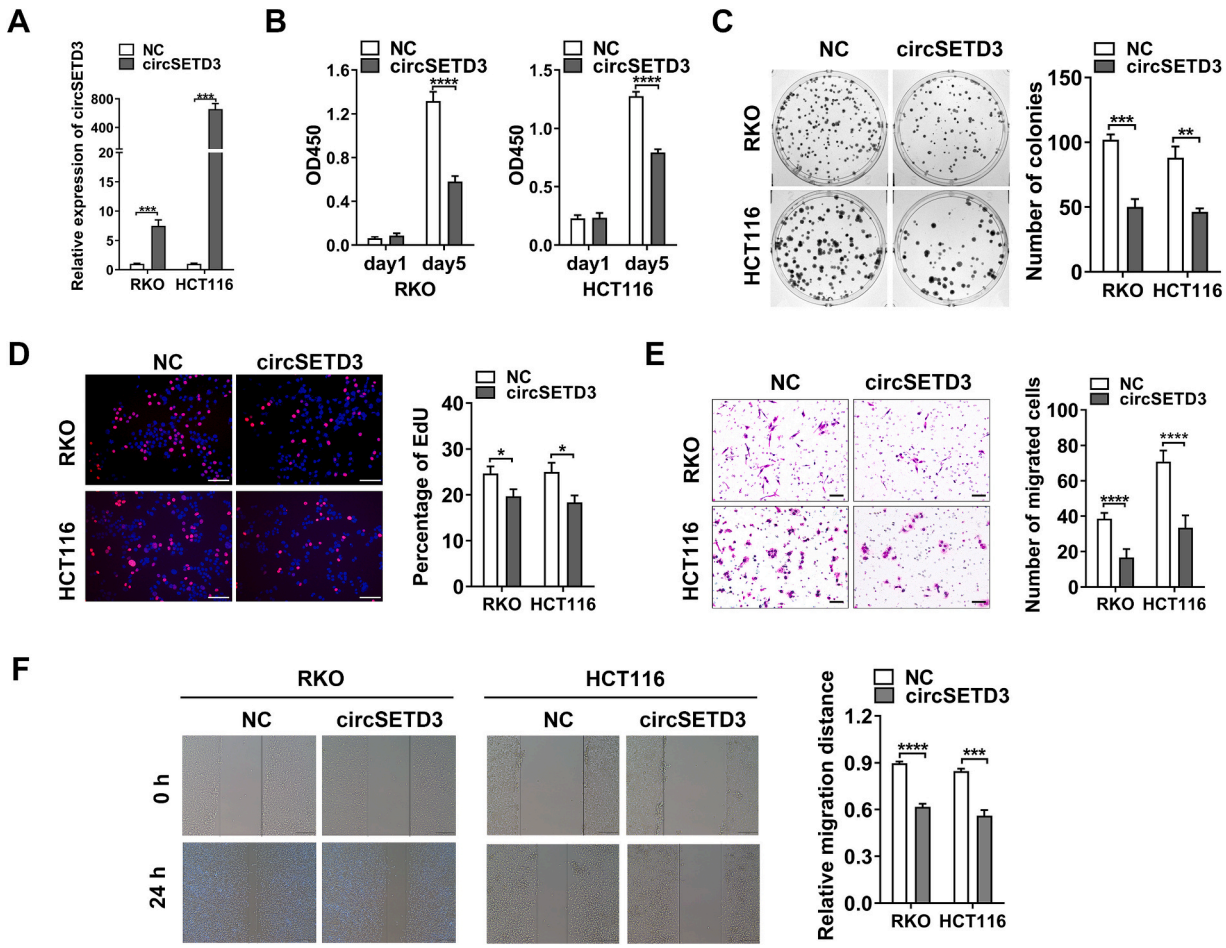


**Fig. 3.** Overexpression of circSETD3 inhibits CRC cell proliferation and migration A) RT-qPCR showed that circSETD3 was upregulated in CRC cells by circSETD3 overexpression vector. B) CCK8 revealed that circSETD3 overexpression restrained CRC cell proliferation. C) Colony formation assay showed that the increased circSETD3 expression decreased the number of colonies. D) EdU staining indicated that the elevated circSETD3 expression reduced the proliferation of CRC cells. E) The Transwell assay demonstrated that the increased circSETD3 expression suppressed the motion of CRC cells. F) The wound healing assay showed the upregulated circSETD3 expression decreased the migration distance of CRC cells.

circSETD3 expression in CRC activates the ErbB3/Akt pathway.

### 3.5. Akt upregulates ErbB3 transcription via HIF1A, forming a positive ErbB3/Akt feedback loop

Given that ErbB3 was upregulated upon circSETD3 knockdown and functioned upstream of the AKT pathway, we further investigated the molecular mechanisms governing its elevated expression. Particularly, we investigated whether HIF1A regulates ErbB3 expression in CRC because it is a transcriptional activator of ErbB3 in head and neck squamous cell carcinomas [20]. Knockdown of HIF1A in CRC cells significantly reduced ErbB3 mRNA levels (Fig. 5A), suggesting a potential transcriptional regulatory relationship. Bioinformatics analysis further identified a putative HIF1A binding site within the ErbB3 promoter region (Fig. 5B). Consequently, we performed a ChIP assay, followed by PCR and RT-qPCR to validate direct binding between HIF1A and ErbB3 promoter. The results demonstrated specific enrichment of the HIF1A-binding sequence in the anti-HIF1A group, confirming the direct interaction of HIF1A with the ErbB3 promoter in CRC (Fig. 5C). Notably, the involvement of the HIF1A pathway (KEGG database, map04066) indicates that Akt enhances HIF1A translation via mTOR. Therefore, we treated CRC cells with an Akt pathway inhibitor (artemisinin), which downregulated ErbB3 expression, but did not affect EGFR expression (Fig. 5D). These findings demonstrate that while ErbB3 activates the AKT pathway, AKT reciprocally promotes ErbB3 transcription through HIF1A, thereby establishing a self-reinforcing ErbB3/Akt positive feedback loop in CRC.

### 3.6. circSETD3 interrupts the ErbB3/Akt feedback loop via the miR-4667-5p/RASA4 axis in CRC

The subcellular location of circSETD3 was determined using FISH to elucidate the detailed mechanism by which circSETD3 inactivates the ErbB3/Akt pathway because the circRNA functions are related to different subcellular locations. The results showed that circSETD3 was mainly located in the cytoplasm of the CRC cells (Fig. 6A). Given the well-characterized role of cytoplasmic circular RNAs as miRNA sponges that bind to target miRNAs via sequence-specific base pairing, we used three bioinformatics databases to predict candidate miRNAs complementary to circSETD3. Seven miRNAs were identified in all databases (Fig. 6B). Furthermore, a circSETD3 luciferase vector was established and a dual-luciferase reporter assay was performed to identify the miRNAs that bind to circSETD3. The results indicated that the miR-4667-5p, miR-4741, miR-1289, and miR-1914-3p mimics reduced luciferase activity in CRC cells (Fig. 6C). Moreover, western blotting showed that miR-4667-5p, miR-4741, and miR-1914-3p mimics activated the ErbB3/Akt pathway, among which miR-4667-5p mimic had the greatest ability to upregulate ErbB3 and p-Akt levels in RKO and HCT116 cells. Thus, miR-4667-5p was the most probable target mediating the effects of circSETD3 on CRC progression (Fig. 6D). Therefore,

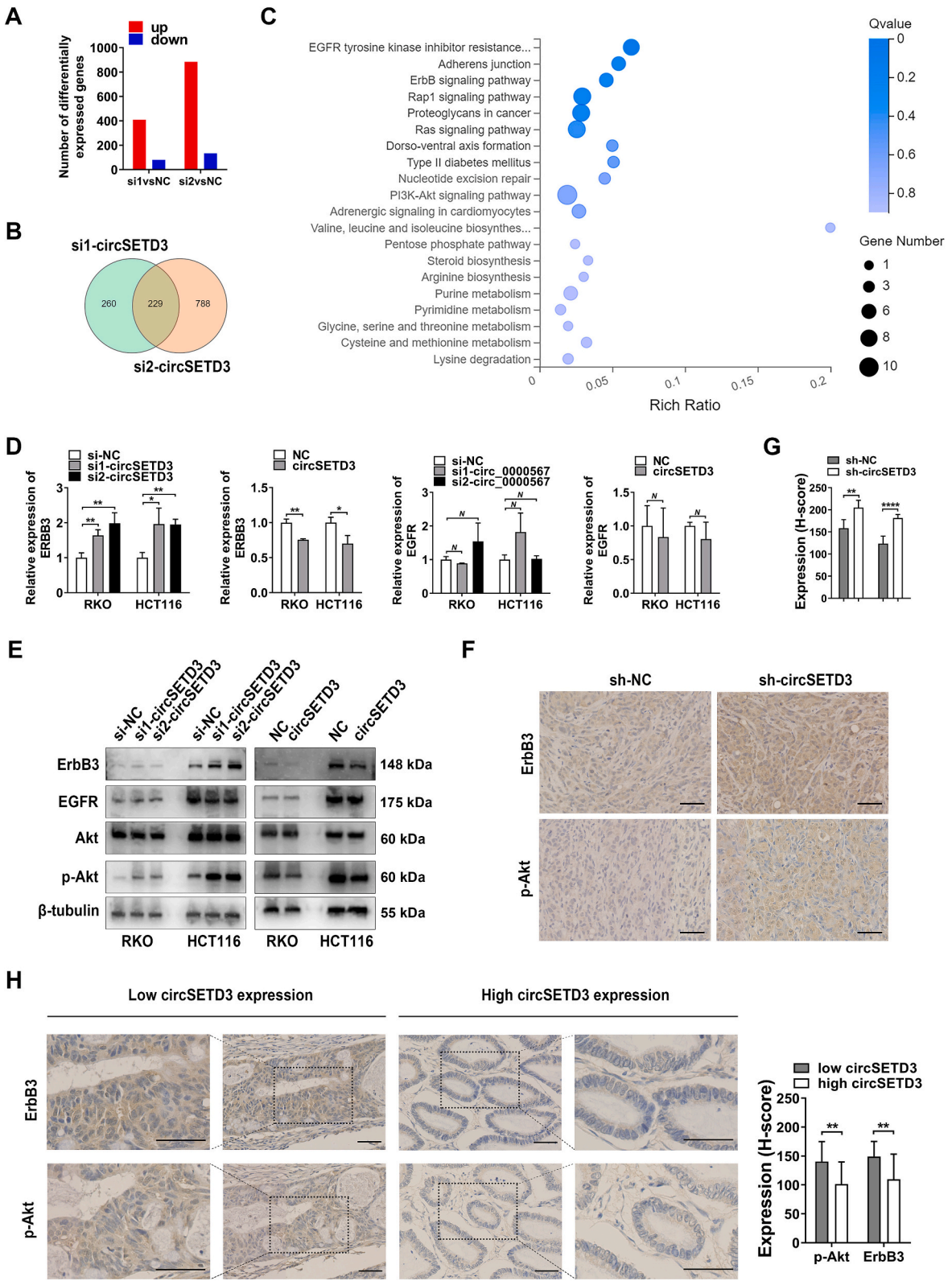


**Fig. 4.** Knockdown of circSETD3 triggers the ErbB3/Akt activation.
A) The number of differentially expressed genes in CRC cells induced by two siRNAs targeting circSETD3. B) In total, 229 differentially expressed genes overlapped between the two siRNA-circSETD3 groups. C) Kyoto Encyclopedia of Genes and Genomes (KEGG) enrichment analysis based on the above mentioned 229 differential expressed genes. D) RT-qPCR results revealed that ErbB3 expression was negatively regulated by circSETD3, whereas EGFR expression was not affected by knockdown or overexpression of circSETD3 in CRC cells. E) Western blot detected the expression level of the indicated proteins. F) and G) IHC staining demonstrated that the ErbB3 and p-Akt levels were increased in the subcutaneous tumors with stable knockdown of circSETD3 expression, Scale bars: 50 μm. H) IHC staining showed that p-Akt and ErbB3 expression was higher in the low circSETD3 expression group ($n = 18$) than that in the high circSETD3 expression group (n = 18). Scale bars:100 μm.

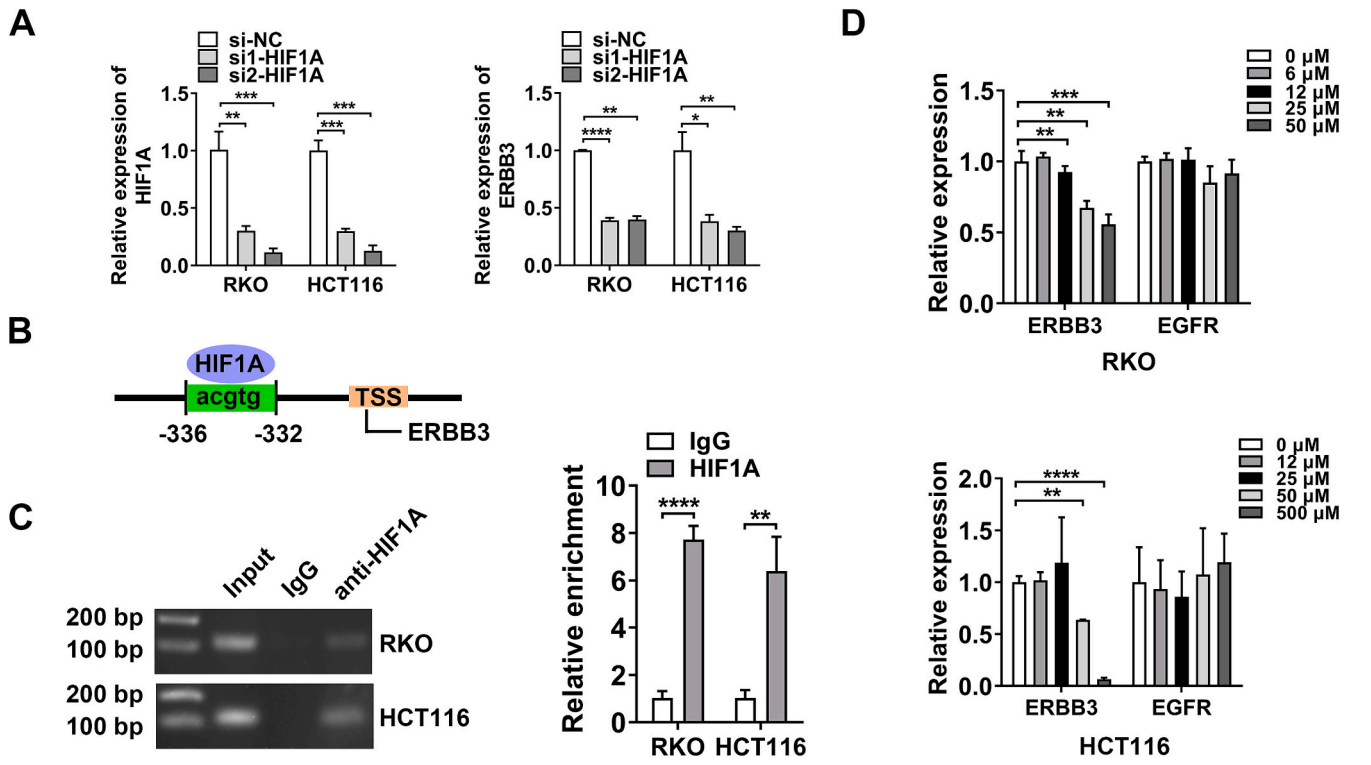


**Fig. 5.** Akt pathway upregulates ErbB3 transcription.
A) RT-qPCR showed that ErbB3 mRNA was downregulated in CRC cells after HIF1A knockdown using siRNAs targeting HIF1A. B) Schematic diagram showed the binding site of HIF1A in the promoter region of ErbB3. C) ChIP, PCR and RT-qPCR assays indicated that using anti-HIF1A antibody could pulldown the DNA fragment of ErbB3 promoter containing the putative binding site of HIF1A. D) ErbB3 expression was downregulated, while EGFR expression was not affected in RKO and HCT116 cells after treatment with artemisinin 24 h.

we constructed a circSETD3 overexpression vector with mutations at the miR-4667-5p binding site to further validate that circSETD3 exerts its function by sequence-specific binding to miR-4667-5p (Fig. S3). Rescue experiments demonstrated that while wild-type circSETD3 overexpression reversed miR-4667-5p-induced upregulation of ErbB3 and p-Akt, the mutant vector failed to rescue these effects (Fig. 6E), establishing a sequence-specific requirement for circSETD3-mediated miRNA sponging. Furthermore, FISH confirmed the cytoplasmic colocalization of circSETD3 and miR-4667-5p in CRC cells (Fig. 6F). Collectively, these results demonstrate that circSETD3 negatively regulates the ErbB3/Akt pathway via the direct sequence-dependent sequestration of miR-4667-5p.

Thereafter, three databases were used to screen the targets of miR-4667-5p, which indicated six potential genes as targets of miR-4667-5p (Fig. 6G). Among them, only Ras p21 protein activator 4 (RASA4) was upregulated in CRC tissues according to the GEPIA database (Fig. S4). Therefore, RASA4 was selected for subsequent experiments. We constructed a RASA4 3'UTR wild and mutant binding sequence luciferase vector (WT1-WT3, MUT1-MUT3) according to the five binding sites of miR-4667-5p in RASA4 3'UTR region (Fig. S5). A subsequent dual-luciferase reporter assay revealed that miR-4667-5p mimics could downregulate RASA4-WT2 luciferase activity in RKO and HCT116 cells (Fig. 6H), demonstrating the binding relationship between miR-4667-5p and RASA4 3'UTR. RASA4 inactivates Ras and the downstream Akt pathway by hydrolyzing Ras-GTP to Ras-GDP. Thus, we speculated that the miR-4667-5p/RASA4 axis is involved in the inhibitory role of circSETD3 in the ErbB3/Akt loop. As expected, western blotting showed that miR-4667-5p reduced RASA4 protein levels while upregulating ErbB3 and p-Akt levels, however, this effect was reversed by circSETD3 co-transfection. In contrast, circSETD3 with the mutant miR-4667-5p binding sequence could not rescue the protein levels of RASA4, ErbB3, and p-Akt (Fig. 6I). Furthermore, consistent with the in vitro findings, subcutaneous xenograft tumor immunohistostaining revealed that RASA4 was downregulated in tumors with circSETD3 knockdown (Fig. 6J). Therefore, we performed a rescue assay to confirm the crucial function of the miR-4667-5p–RASA4 axis in the regulation of circSETD3 in CRC progression. EdU and Transwell assays demonstrated that miR-4667-5p mimics or knockdown of RASA4 restored the inhibitory role of circSETD3 in CRC proliferation and migration (Figs. S6 and S7). Together, these data indicated that the miR-4667-5p/RASA4 axis is involved in the regulatory role of circSETD3 in the ErbB3/Akt feedback loop.

### 3.7. *circSETD3 downregulation confers cetuximab resistance in CRC cells*

Cetuximab is a targeted drug against EGFR that competitively blocks ligands from binding to EGFR, thereby inactivating its downstream Ras and Akt pathways to inhibit tumor progression. However, drug resistance limits its clinical efficacy. Studies have revealed that the upregulation of ErbB2 or ErbB3 is an important reason for cetuximab resistance [5–9]. Our findings revealed that reduced circSETD3 expression in CRC cells caused continuous ErbB3 upregulation by activating the ErbB3/Akt feedback loop via the miR-4667-5p/RASA4 axis. Therefore, we hypothesized that downregulation of circSETD3 in CRC may contribute to cetuximab resistance.

Consequently, a CCK8 assay was performed to detect the growth inhibition rate of CRC cells treated with cetuximab. The results showed that circSETD3 knockdown weakened the inhibitory effect of cetuximab on CRC cell growth, whereas, circSETD3 overexpression enhanced the growth inhibition rate of cetuximab in CRC cells (Fig. 7A). Subsequently, apoptotic markers were detected by western blotting to evaluate the effect of circSETD3 on cetuximab-induced apoptosis. As shown in Fig. 7B, decreased circSETD3 expression reduced the levels of the apoptotic marker cleaved caspase3 and cleaved PARP, whereas

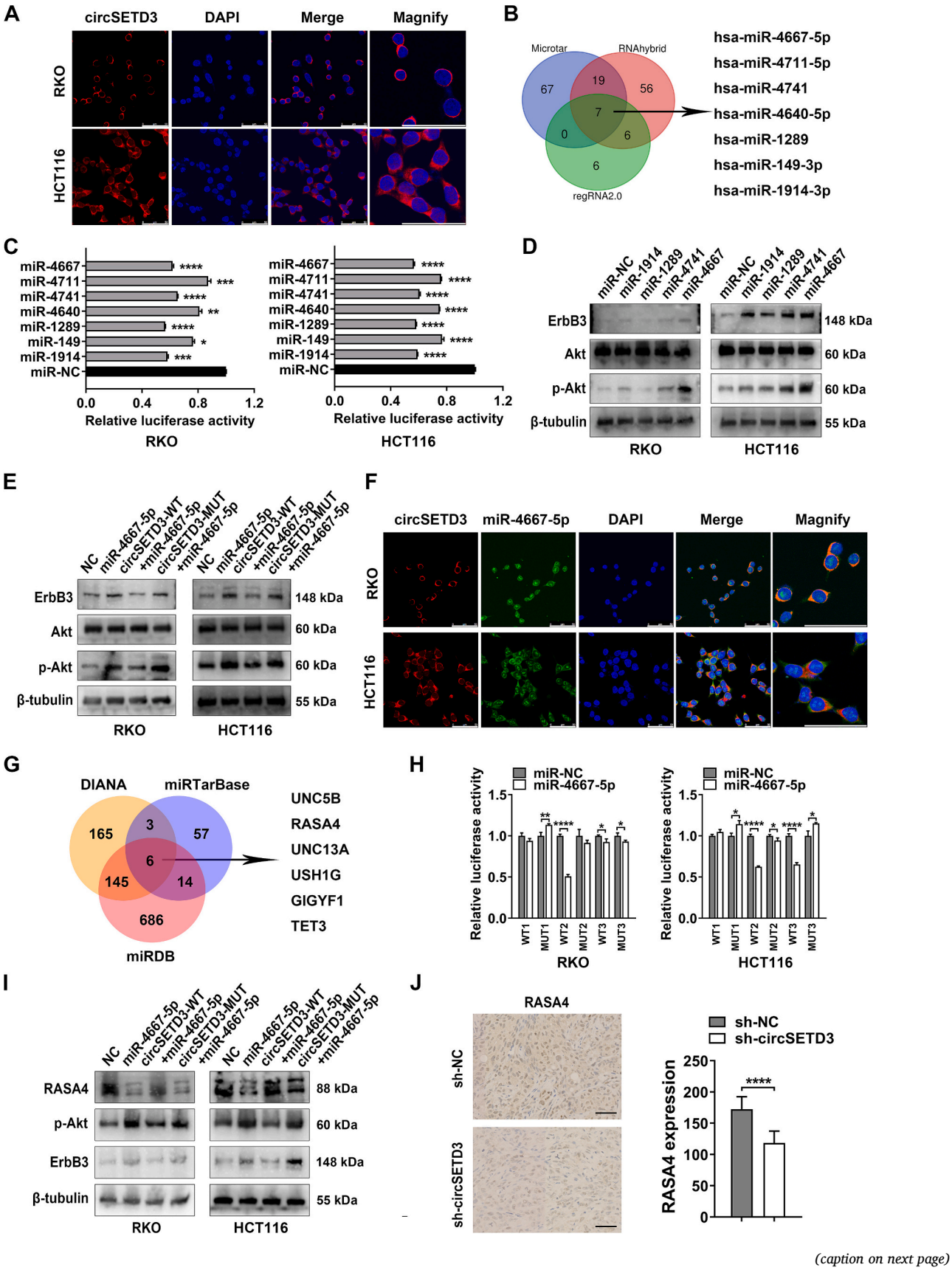


*(caption on next page)*

**Fig. 6.** miR-4667-5p/RASA4 axis is involved in the regulatory role of circSETD3 in the ErbB3/Akt feedback loop.
A) The subcellular location of circSETD3 in CRC cells was detected using FISH assay. Scale bars: 50 μm. B) The seven miRNAs that circSETD3 binds to were predicted using the indicated three databases. C) Dual-luciferase assays showed that miR-4667-5p, miR-4741, miR-1289, and miR-1914-3p mimics could reduce the luciferase activity in CRC cells after transfection with circSETD3 luciferase vectors. D) The expression of ErbB3, Akt and p-Akt in CRC cells was determined by western blotting after treatment with the indicated four miRNA mimics. E) Western blotting detected ErbB3, Akt and p-Akt levels in CRC cells after transfected miR-4667-5p mimics with or without circSETD3 overexpression vector (circSETD3-WT) or circSETD3 vector with mutant binding site of miR-4667-5p (circSETD3-MUT). F) FISH indicated the co-localization of circSETD3 and miR-4667-5p in the cytoplasm of CRC cells. Scale bars: 50 μm. G) The six indicated target genes of miR-4667-5p were predicted using the three databases. H) Dual-luciferase assays showed that the relative luciferase activity of CRC cells after transfection with miR-4667-5p and RASA4 3'UTR luciferase WT or MUT vectors. I) RASA4, p-Akt and ErbB3 expression was detected in CRC cells after transfection with miR-4667-5p with or without the above mentioned circSETD3 overexpression vector or vector with mutant binding site of miR-4667-5p. J) The expression of RASA4 in nude mice subcutaneous tumors with stable knockdown of circSETD3 expression was lower than that in the control group.

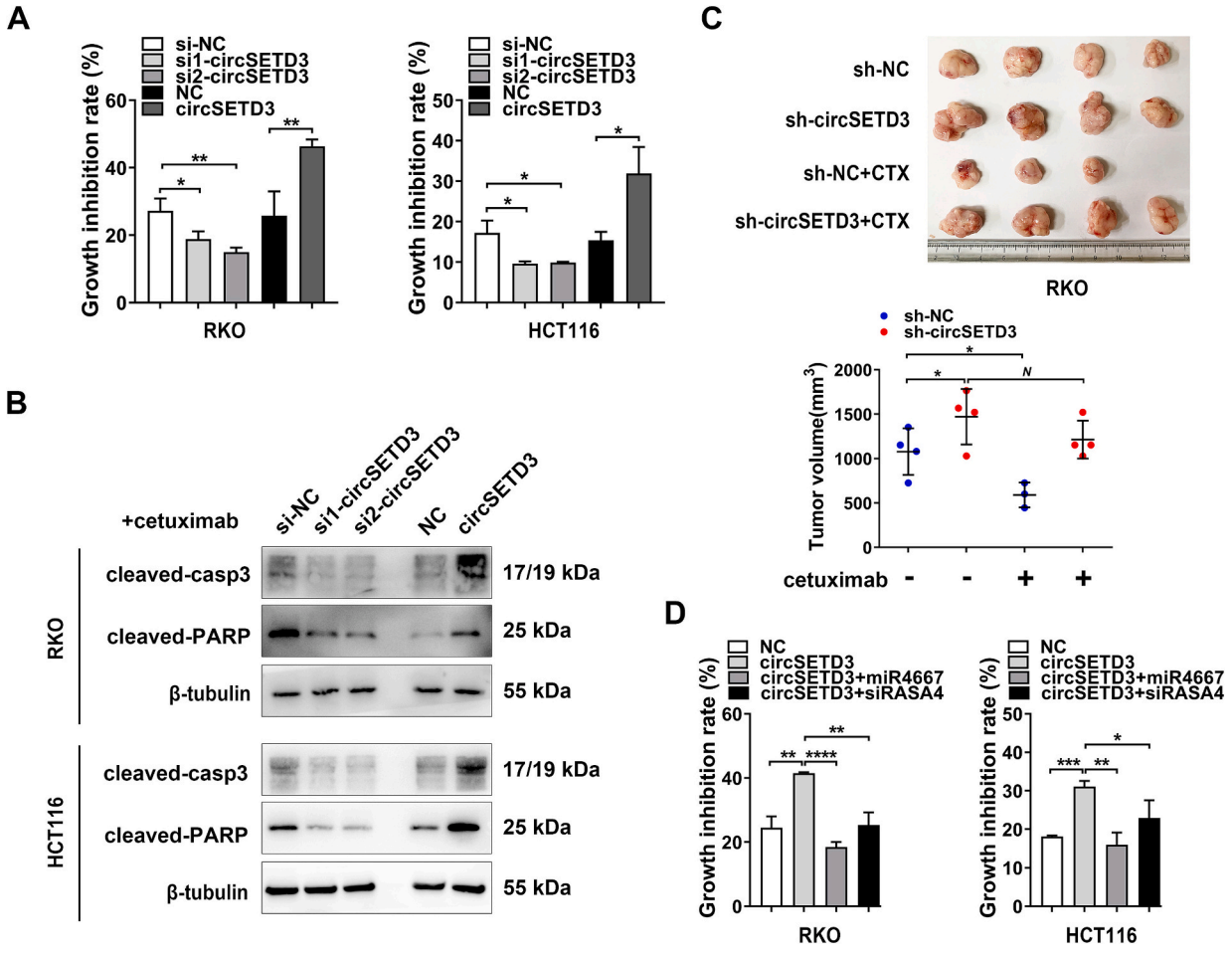


**Fig. 7.** circSETD3 enhances the sensitivity of CRC cells to cetuximab.
A) A CCK8 assay demonstrated that circSETD3 knockdown antagonized the inhibitory effect of cetuximab (500 μg/mL for 48 h) on CRC cell growth, while circSETD3 overexpression enhanced the cetuximab growth inhibition rate on CRC cells. B) Western blotting was performed to detect the apoptotic markers expression in the CRC cells with decreased or increased circSETD3 expression after treatment with cetuximab (500 μg/mL for 48 h). C) The growth of subcutaneous tumors with stable knockdown of circSETD3 expression was not affected by cetuximab treatment, whereas tumors growing from control cells were suppressed by cetuximab treatment ($n = 4$). D) Rescue assay showed that miR-4667-5p mimics and siRNA targeting to RASA4 could restore the sensitive-enhancing role of circSETD3 on CRC cells with cetuximab treatment.

increased circSETD3 expression increased their levels (Fig. 7B). Consistent with the in vitro findings, the in vivo therapeutic experiments also indicated that downregulation of circSETD3 reduced the sensitivity of CRC cells to cetuximab treatment (Fig. 7C). Therefore, we performed a rescue assay to verify whether the miR4667-5p/RASA4 axis is involved in the regulatory role of circSETD3 in CRC cells in response to cetuximab treatment. The CCK8 assay showed that miR-4667-5p mimics and siRNA targeting RASA4 restored the sensitivity-enhancing role of circSETD3 in CRC cells treated with cetuximab (Fig. 7D). Overall, these results indicate that circSETD3 enhances the sensitivity of CRC cells to cetuximab.

### *3.8. Exosomal circSETD3 uptake by CRC cells suppresses the ErbB3/Akt feedback loop*

Recent studies using engineered extracellular vesicles carrying miRNAs for pancreatic cancer treatment have established promising platforms for noncoding RNA-based targeted therapies [21]. Therefore, we conducted preliminary experiments to explore the therapeutic potential of circSETD3 in CRC progression and cetuximab resistance.

Bioinformatics analysis using exoRBase (http://www.exorbase.org/) revealed detectable levels of circSETD3 in plasma exosomes from healthy individuals and patients with CRC, suggesting active cellular

secretion of circSETD3. Therefore, we generated circSETD3-enriched exosomes from HCT116 cells transfected with a circSETD3 overexpression vector, which were then added to CRC cells to assess their effects on the ErbB3/Akt pathway, to investigate functional delivery (Fig. 8A). Transmission electron microscopy (TEM) confirmed the bilayer membrane structure of the exosomes, and nanoparticle tracking analysis (NAT) showed that the size distribution of the exosomes was approximately 200 nm (Fig. 8B and C). Additionally, western blotting confirmed the presence of the exosome-specific markers CD9, CD63, and TSG101 and the absence of the negative marker calnexin in exosomes (Fig. 8D). These experiments characterized exosomes isolated from the culture medium of HCT116 cells overexpressing circSETD3.

Moreover, RT-qPCR confirmed the significant enrichment of circSETD3 in exosomes derived from the culture medium of HCT116 cells overexpressing circSETD3 (Fig. 8E). Subsequent treatment of RKO and HCT116 cells with circSETD3-enriched exosomes resulted in successful intracellular delivery, as evidenced by elevated circSETD3 levels (Fig. 8F). Furthermore, western blot analysis demonstrated that exosomal circSETD3 treatment upregulated RASA4 expression and downregulated p-Akt and ErbB3 expression in both cell lines (Fig. 8G). These collective findings establish that exogenous exosome-mediated circSETD3 delivery effectively disrupts the ErbB3/Akt feedback loop via the miR-4667-5p/RASA4 axis.

## 4. Discussion

We previously reported that circSETD3 is downregulated in CRC tissues and is related to tumor size, metastasis, and TNM state [15]. Building on these results, in the current study, we demonstrated that circSETD3 functions as a tumor suppressor in CRC, effectively inhibiting CRC growth and metastasis and enhancing cetuximab sensitivity in vitro and in vivo. In addition, we identified a novel positive feedback loop between ErbB3 and Akt that drives CRC progression and cetuximab resistance. Notably, our results revealed that circSETD3 downregulation in CRC leads to reduced RASA4 expression via miR-4667-5p, a critical event that triggers the activation of the ErbB3/Akt feedback loop (Fig. 9). Thus, our results suggest that restoration of circSETD3 represents a promising strategy for suppressing CRC progression and overcoming cetuximab resistance.

In recent years, dysregulated circSETD3 has been detected in a diverse range of cancers and which regulates the progression of malignancies; however, its role and mechanism of action in CRC remained unclear. In this study, we demonstrated that the downregulation of circSETD3 in CRC is essential for malignant progression and is related to poor patient prognosis. Our results are consistent with previous studies which reported that circSETD3 was downregulated and inhibited cancer growth and metastasis in hepatoblastoma [16], cholangiocarcinoma [17], bladder cancer [18], and hepatocellular carcinoma [19]. In contrast, circSETD3 functioned as an oncogene to promote

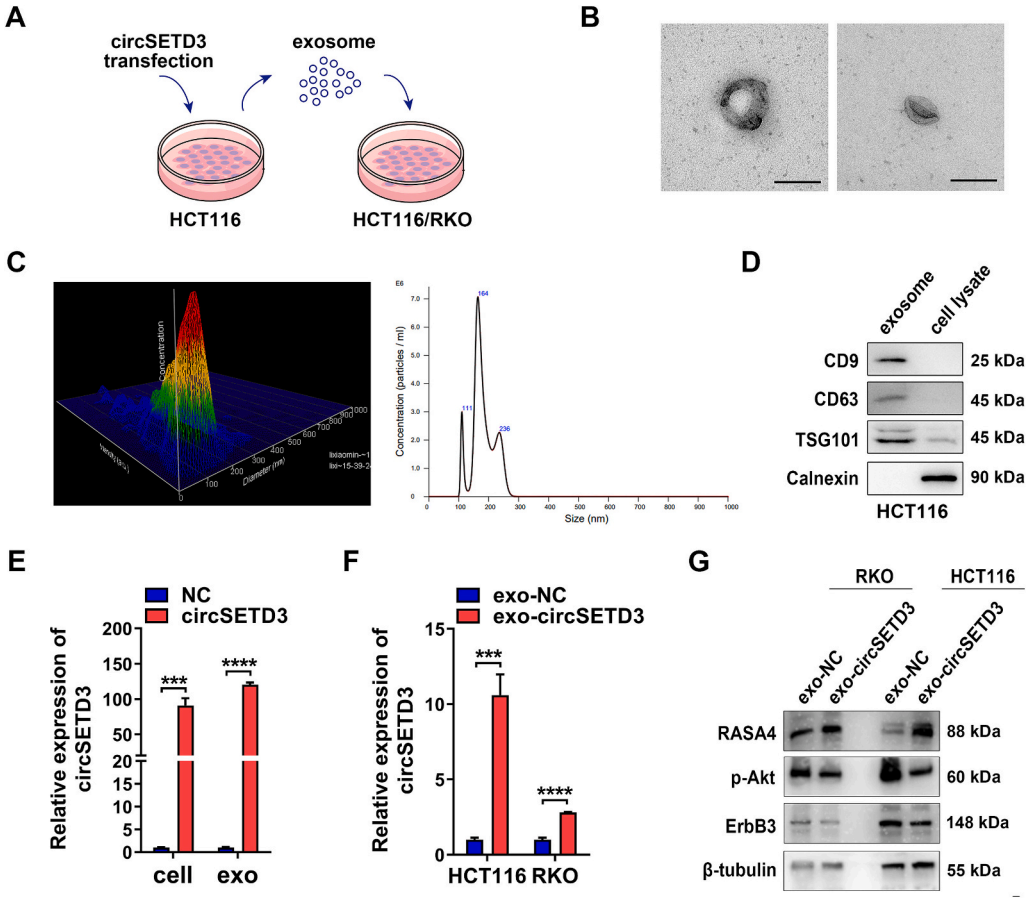


**Fig. 8.** Exosomal circSETD3 suppresses the ErbB3/Akt feedback loop.
A) The schematic diagram of the production, isolation, and application of circSETD3-rich exosomes. B) Transmission electron microscopy (TEM) was used to elucidate the structure of the exosomes extracted from the culture medium of CRC cells. Scale bars: 200 nm. C) Nanoparticle tracking analysis (NTA) was performed to confirm the size of exosomes. D) Western blotting was used to identify the exosome-specific markers CD9, CD63, TSG101, and negative control marker Calnexin in the exosomes and cell lysate. E) The relative expression of circSETD3 in CRC cells and exosomes isolated from the culture medium of HCT116 cells after transfected with circSETD3 overexpression vector. F) The levels of circSETD3 in RKO and HCT116 cells after treated with exosomes containing high levels of circSETD3. G) RASA4, p-Akt and ErbB3 expression in RKO and HCT116 after treated with the previous circSETD3-rich exosomes 24 h.

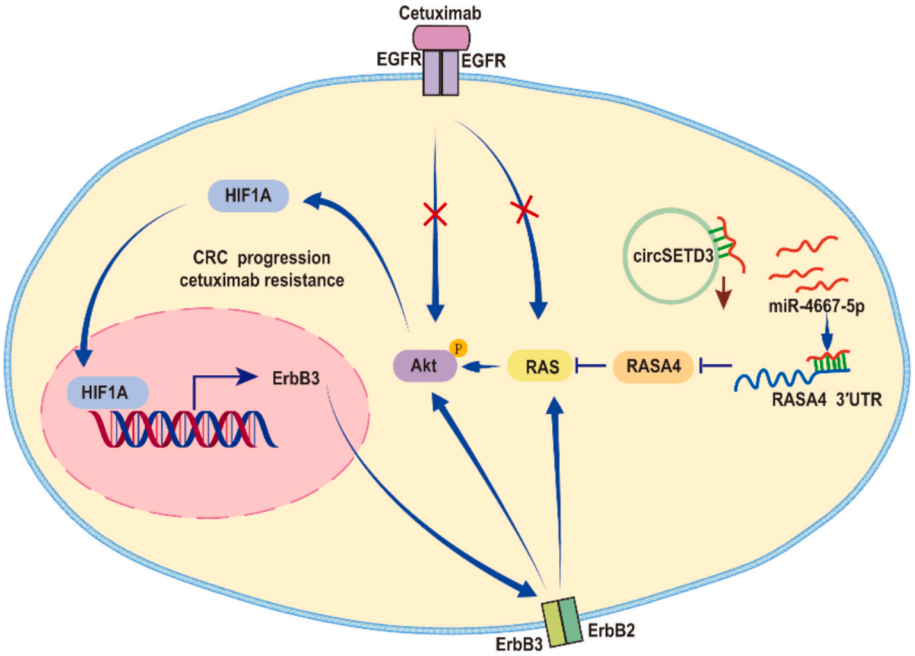


**Fig. 9.** Mechanistic model of circSETD3 downregulation-mediated promotion of CRC progression and cetuximab resistance.

nasopharyngeal carcinoma proliferation, migration and cisplatin resistance [22,23]. Thus, the dual function of circSETD3 in different cancers may be related to different downstream miRNAs and their targets.

In the current study, our results revealed that circSETD3 sponges miR-4667-5p to upregulate its target, RASA4, in CRC. RASA4 is a member of the Ras GTPase-activating protein family (RAS-GAPs). As a natural Ras inhibitor, RASA4 inactivates Ras and the downstream Akt pathway by hydrolyzing active Ras-GTP to inactive Ras-GDP [24]. However, RASA4 is often expressed at lower levels in cancers because of methylation of the promoter region or post-transcriptional regulation, which causes the continuous activation of Ras and its downstream Akt and MAPK pathways, thus promoting the malignant progression of cancers and drug resistance. For instance, RASA4 is downregulated in cervical squamous cell carcinoma and promotes cell proliferation by activating Ras [25]. Similarly, RASA4 inhibits tumor cell proliferation and promotes apoptosis by suppressing the RAS/MAPK pathway in triple-negative breast cancer [26]. However, the mechanisms underlying the downregulation of RASA4 in tumors remain unclear. In this regard, we found that circSETD3 was downregulated in CRC and attenuated its sponging effect on miR-4667-5p, thereby releasing miR-4667-5p and downregulating RASA4 expression. This may represent a key mechanism underlying RASA4 downregulation in CRC.

Previous studies have established that ErbB3 heterodimerizes with ErbB2 to initiate Ras activation and subsequent activation of downstream MAPK/ERK and PI3K/Akt pathways [27–30]. Building on this foundation, our current study revealed that Akt-mediated regulation enhances ErbB3 transcription via HIF1A, thereby establishing a functionally significant positive feedback loop between ErbB3 and Akt signaling in CRC. This self-reinforcing ErbB3/Akt feedback loop drives tumor progression and confers cetuximab resistance in CRC. Notably, our results demonstrated that circSETD3 serves as a critical modulator of this feedback loop via the miR-4667-5p/RASA4 axis. Consistent with previous reports implicating ErbB2/3 upregulation in cetuximab resistance, circSETD3 knockdown significantly diminished cetuximab sensitivity in cellular and animal models. Moreover, we demonstrated that exosomal circSETD3 delivery effectively suppressed the ErbB3/Akt feedback loop by restoring RASA4 expression. Collectively, these findings indicate that exogenous circSETD3 supplementation represents a promising therapeutic approach for simultaneously inhibiting CRC progression and restoring cetuximab sensitivity.

In conclusion, our study revealed a novel positive feedback loop between ErbB3 and Akt in CRC, wherein Akt upregulates ErbB3 transcription by enhancing HIF1A translation, while ErbB3 reciprocally activates the AKT pathway. This feedback loop drives sustained ErbB3 overexpression and the activation of the Akt pathway, ultimately promoting CRC progression and conferring cetuximab resistance. Notably, the downregulation of circSETD3 was the pivotal trigger for this feedback loop, which is mediated by the miR-4667-5p/RASA4 regulatory axis. Additionally, our study demonstrated that exogenous circSETD3 supplementation may serve as a promising therapeutic strategy for CRC, as it effectively inhibits CRC progression and restores cetuximab sensitivity by suppressing the ErbB3/Akt feedback activation loop. Consequently, our findings provide a foundation for future clinical applications. However, further studies using animal models or organoids derived from CRC tissues are required to elucidate the role of circSETD3 overexpression in CRC progression and cetuximab resistance, as well as the functions and mechanisms of nuclear and cytoplasmic miR-4667-5p in CRC progression. Moreover, in the current study, we used a circSETD3 overexpression vector to produce exosomes that enriched circSETD3, and preliminarily found that CRC cells could absorb exosomal circSETD3 to suppress the ErbB3/Akt pathway. Therefore, further functional experiments in vitro and in vivo should be performed for the application of circSETD3 using engineered circular RNA production technology.

Supplementary data to this article can be found online at https://doi.org/10.1016/j.ijbiomac.2025.145352.

## CRediT authorship contribution statement

**Xiaomin Li:** Writing – review & editing, Writing – original draft, Funding acquisition, Data curation. **Tao Chen:** Funding acquisition, Formal analysis. **Yujie Cai:** Writing – review & editing, Validation. **Jingtao Zhang:** Formal analysis. **Yuxin Wang:** Validation. **Jianjun Wang:** Writing – review & editing, Funding acquisition. **Xueyuan Mao:** Validation. **Liancheng Xu:** Formal analysis. **Dongdong Li:** Writing – review & editing. **Yu Wang:** Formal analysis. **Xiaoyan Wang:** Writing – review & editing, Supervision, Project administration, Investigation, Funding acquisition, Conceptualization.

## Declaration of competing interest

The authors declare that they have no known competing financial interests or personal relationships that could have appeared to influence the work reported in this paper.

## Acknowledgements

This work was supported by Suqian Sci&Tech Program (Grant Number: KY202404, KY202304), The Social Development Projects of Key R&D Programs in Xuzhou city (Grant Number: KC23247), Suqian Talent Xiongying Plan Project (Grant Number: SQXY202436), National Natural Science Foundation of China (Grant Number: 81902479), Key project fund of Jiangsu Provincial Health Commission (Grant Number: ZD2022052), Guangdong Basic and Applied Basic Research Foundation (Grant Number: 2021A1515010665), Natural Science Foundation of the Anhui provincial High-Education Institutions of China (Grant Number: KJ2021A0828), and China Postdoctoral Science Foundation (Grant Number: 2019M652961).

## Data availability

The data that support the findings of this study are available from the corresponding author upon reasonable request.

## References

[1] H. Sung, J. Ferlay, R.L. Siegel, M. Laversanne, I. Soerjomataram, A. Jemal, et al., Global cancer statistics 2020: GLOBOCAN estimates of incidence and mortality worldwide for 36 cancers in 185 countries, CA Cancer J. Clin. (2021), https://doi.org/10.3322/caac.21660.

[2] A. Lièvre, B. Ouine, J. Canet, A. Cartier, Y. Amar, W. Cacheux, et al., Protein biomarkers predictive for response to anti-EGFR treatment in RAS wild-type metastatic colorectal carcinoma, Br. J. Cancer 117 (12) (2017) 1819–1827, https://doi.org/10.1038/bjc.2017.353.

[3] P.D. Bonomi, D. Gandara, F.R. Hirsch, K.M. Kerr, C. Obasaju, L. Paz-Ares, et al., Predictive biomarkers for response to EGFR-directed monoclonal antibodies for advanced squamous cell lung cancer, Ann. Oncol. 29 (8) (2018) 1701–1709, https://doi.org/10.1093/annonc/mdy196.

[4] E. Martinelli, D. Ciardiello, G. Martini, T. Troiani, C. Cardone, P.P. Vitiello, et al., Implementing anti-epidermal growth factor receptor (EGFR) therapy in metastatic colorectal cancer: challenges and future perspectives, Ann. Oncol. 31 (1) (2020) 30–40, https://doi.org/10.1016/j.annonc.2019.10.007.

[5] K. Yonesaka, HER2-/HER3-targeting antibody-drug conjugates for treating lung and colorectal cancers resistant to EGFR inhibitors, Cancers (Basel) 13 (5) (2021), https://doi.org/10.3390/cancers13051047.

[6] L.C. Conradi, M. Spitzner, A.L. Metzger, M. Kisly, P. Middel, H. Bohnenberger, et al., Combined targeting of HER-2 and HER-3 represents a promising therapeutic strategy in colorectal cancer, BMC Cancer 19 (1) (2019) 880, https://doi.org/10.1186/s12885-019-6051-0.

[7] S. Temraz, D. Mukherji, A. Shamseddine, Dual targeting of HER3 and EGFR in colorectal tumors might overcome anti-EGFR resistance, Crit. Rev. Oncol. Hematol. 101 (2016) 151–157, https://doi.org/10.1016/j.critrevonc.2016.03.009.

[8] S.A. Khelwatty, S. Essapen, A.M. Seddon, Z. Fan, H. Modjtahedi, Acquired resistance to anti-EGFR mAb ICR62 in cancer cells is accompanied by an increased EGFR expression, HER-2/HER-3 signalling and sensitivity to pan HER blockers, Br. J. Cancer 113 (7) (2015) 1010–1019, https://doi.org/10.1038/bjc.2015.319.

[9] L. Zhang, C. Castanaro, B. Luan, K. Yang, L. Fan, J.L. Fairhurst, et al., ERBB3/HER2 signaling promotes resistance to EGFR blockade in head and neck and colorectal cancer models, Mol. Cancer Ther. 13 (5) (2014) 1345–1355, https://doi.org/10.1158/1535-7163.mct-13-1033.

[10] X. Li, J. Wang, W. Lin, Q. Yuan, Y. Lu, H. Wang, et al., circEXOC6B interacting with RRAGB, an mTORC1 activator, inhibits the progression of colorectal cancer by antagonizing the HIF1A-RRAGB-mTORC1 positive feedback loop, Mol. Cancer 21 (1) (2022) 135, https://doi.org/10.1186/s12943-022-01600-1.

[11] X. Li, J. Wang, C. Zhang, C. Lin, J. Zhang, W. Zhang, et al., Circular RNA circITGA7 inhibits colorectal cancer growth and metastasis by modulating the Ras pathway and upregulating transcription of its host gene ITGA7, J. Pathol. 246 (2) (2018) 166–179, https://doi.org/10.1002/path.5125.

[12] S. Wei, W. Hu, J. Feng, Y. Geng, Promotion or remission: a role of noncoding RNAs in colorectal cancer resistance to anti-EGFR therapy, Cell Commun. Signal 20 (1) (2022) 150, https://doi.org/10.1186/s12964-022-00960-x.

[13] Y. Geng, X. Zheng, D. Zhang, S. Wei, J. Feng, W. Wang, et al., CircHIF1A induces cetuximab resistance in colorectal cancer by promoting HIF1α-mediated glycometabolism alteration, Biol. Direct 19 (1) (2024) 36, https://doi.org/10.1186/s13062-024-00478-x.

[14] Q. Zhang, Y. Zheng, J. Liu, X. Tang, Y. Wang, X. Li, et al., CircIFNGR2 enhances proliferation and migration of CRC and induces cetuximab resistance by indirectly targeting KRAS via sponging to MiR-30b, Cell Death Dis. 14 (1) (2023) 24, https://doi.org/10.1038/s41419-022-05536-8.

[15] J. Wang, X. Li, L. Lu, L. He, H. Hu, Z. Xu, Circular RNA hsa_circ_0000567 can be used as a promising diagnostic biomarker for human colorectal cancer, J. Clin. Lab. Anal. 32 (5) (2018) e22379, https://doi.org/10.1002/jcla.22379.

[16] X. Li, H. Wang, Z. Liu, A. Abudureyimu, CircSETD3 (Hsa_circ_0000567) suppresses hepatoblastoma pathogenesis via targeting the miR-423-3p/Bcl-2-interacting mediator of cell death axis, Front. Genet. 12 (2021) 724197, https://doi.org/10.3389/fgene.2021.724197.

[17] W. Xiong, A. Zhang, X. Xiao, W. Liu, CircSETD3 (hsa_circ_0000567) inhibits proliferation and induces apoptosis in cholangiocarcinoma cells via downregulation of microRNA-421 expression, Bioengineered 13 (4) (2022) 10191–10201, https://doi.org/10.1080/21655979.2022.2061283.

[18] Y. Tian, P. Gao, D. Dai, L. Chen, X. Chu, X. Mei, Circular RNA circSETD3 hampers cell growth, migration, and stem cell properties in bladder cancer through sponging miR-641 to upregulate PTEN, Cell Cycle 20 (16) (2021) 1589–1602, https://doi.org/10.1080/15384101.2021.1954758.

[19] L. Xu, X. Feng, X. Hao, P. Wang, Y. Zhang, X. Zheng, et al., CircSETD3 (Hsa_circ_0000567) acts as a sponge for microRNA-421 inhibiting hepatocellular carcinoma growth, J. Exp. Clin. Cancer Res. 38 (1) (2019) 98, https://doi.org/10.1186/s13046-019-1041-2.

[20] J.O. Humtsoe, E. Pham, R.J. Louie, D.A. Chan, R.H. Kramer, ErbB3 upregulation by the HNSCC 3D microenvironment modulates cell survival and growth, Oncogene 35 (12) (2016) 1554–1564, https://doi.org/10.1038/onc.2015.220.

[21] P. Zhou, X. Du, W. Jia, K. Feng, Y. Zhang, Engineered extracellular vesicles for targeted reprogramming of cancer-associated fibroblasts to potentiate therapy of pancreatic cancer, Signal Transduct. Target. Ther. 9 (1) (2024) 151, https://doi.org/10.1038/s41392-024-01872-7.

[22] L. Tang, W. Xiong, L. Zhang, D. Wang, Y. Wang, Y. Wu, et al., circSETD3 regulates MAPRE1 through miR-615-5p and miR-1538 sponges to promote migration and invasion in nasopharyngeal carcinoma, Oncogene 40 (2) (2021) 307–321, https://doi.org/10.1038/s41388-020-01531-5.

[23] G. Deng, F. Wang, Y. Song, Circular RNA SET domain protein 3 promotes nasopharyngeal carcinoma proliferation, cisplatin resistance, and protein kinase B / mammalian target of rapamycin pathway activation by modulating microRNA-147a expression, Bioengineered 13 (3) (2022) 5843–5854, https://doi.org/10.1080/21655979.2022.2036907.

[24] P. Gao, S. Liu, R. Yoshida, C.Y. Shi, S. Yoshimachi, N. Sakata, et al., Ral GTPase activation by downregulation of RalGAP enhances oral squamous cell carcinoma progression, J. Dent. Res. 98 (9) (2019) 1011–1019, https://doi.org/10.1177/0022034519860828.

[25] J. Chen, J. Huang, Q. Huang, J. Li, E. Chen, W. Xu, RASA4 inhibits the HIFα signaling pathway to suppress proliferation of cervical cancer cells, Bioengineered 12 (2) (2021) 10723–10733, https://doi.org/10.1080/21655979.2021.2002499.

[26] Y. Wang, Y.X. Qi, Z. Qi, S.Y. Tsang, TRPC3 Regulates the Proliferation and Apoptosis Resistance of Triple Negative Breast Cancer Cells through the TRPC3/RASA4/MAPK Pathway, Cancers (Basel) 11 (4) (2019), https://doi.org/10.3390/cancers11040558.

[27] E. Capone, T. Tryggvason, I. Cela, B. Dufrusine, M. Pinti, F. Del Pizzo, et al., HER-3 surface expression increases in advanced colorectal cancer representing a potential therapeutic target, Cell Death Discov. 9 (1) (2023) 400, https://doi.org/10.1038/s41420-023-01692-8.

[28] Q. Yan, K. Guo, G. Feng, F. Shan, L. Sun, K. Zhang, et al., Association between the overexpression of Her3 and clinical pathology and prognosis of colorectal cancer: a meta-analysis, Medicine (Baltimore) 97 (37) (2018) e12317, https://doi.org/10.1097/md.0000000000012317.

[29] N. Gaborit, A. Abdul-Hai, M. Mancini, M. Lindzen, S. Lavi, O. Leitner, et al., Examination of HER3 targeting in cancer using monoclonal antibodies, Proc. Natl. Acad. Sci. U. S. A. 112 (3) (2015) 839–844, https://doi.org/10.1073/pnas.1423645112.

[30] F. Lédel, M. Hallström, P. Ragnhammar, K. Öhrling, D. Edler, HER3 expression in patients with primary colorectal cancer and corresponding lymph node metastases related to clinical outcome, Eur. J. Cancer 50 (3) (2014) 656–662, https://doi.org/10.1016/j.ejca.2013.11.008.